Brain, Behavior, and Immunity 118 (2024) 275–286

Contents lists available at ScienceDirect

Brain Behavior and Immunity

journal homepage: www.elsevier.com/locate/ybrbi

Full-length Article

Compartmentalized role of xCT in supporting pancreatic tumor growth, inflammation and mood disturbance in mice

Olaya Lara [a,b,1], Pauline Janssen [a,b,1], Marco Mambretti [b], Laura De Pauw [a], Gamze Ates [a], Liselotte Mackens [a], Jolien De Munck [a], Jarne Walckiers [a], Zhaolong Pan [b], Pauline Beckers [c], Elisa Espinet [d,e], Hideyo Sato [f], Mark De Ridder [g], Daniel L. Marks [h], Kurt Barbé [i], Joeri L. Aerts [a], Emmanuel Hermans [c], Ilse Rooman [b,2,*], Ann Massie [a,2,*]

[a] Laboratory of Neuro-Aging & Viro-Immunotherapy, Center for Neurosciences (C4N), Vrije Universiteit Brussel (VUB), Brussels 1090, Belgium
[b] Laboratory for Medical and Molecular Oncology, Translational Oncology Research Center (TORC), VUB, Brussels 1090, Belgium
[c] Institute of Neuroscience, Université catholique de Louvain, Brussels 1200, Belgium
[d] Pancreatic Cancer Lab, Department of Pathology and Experimental Therapy, School of Medicine, University of Barcelona, L'Hospitalet de Llobregat, Barcelona 08907, Spain
[e] Molecular Mechanisms and Experimental Therapy in Oncology Program, Institut d'Investigació Biomèdica de Bellvitge, L'Hospitalet de Llobregat, Barcelona 08907, Spain
[f] Department of Medical Technology, Niigata University, Niigata 950-3198, Japan
[g] Department of Radiotherapy, UZ Brussels, VUB, Brussels 1090, Belgium
[h] Papé Family Pediatric Research Institute, Oregon Health and Science University, Portland, OR 97239, USA
[i] The Biostatistics and Medical Informatics Department, VUB, Brussels 1090, Belgium

ARTICLE INFO

Keywords:
Cystine/glutamate antiporter system x_c^-
pancreatic cancer
(neuro)inflammation
mood disturbances
cachexia

ABSTRACT

xCT (Slc7a11), the specific subunit of the cystine/glutamate antiporter system x_c^-, is present in the brain and on immune cells, where it is known to modulate behavior and inflammatory responses. In a variety of cancers -including pancreatic ductal adenocarcinoma (PDAC)-, xCT is upregulated by tumor cells to support their growth and spread. Therefore, we studied the impact of xCT deletion in pancreatic tumor cells (Panc02) and/or the host ($xCT^{-/-}$ mice) on tumor burden, inflammation, cachexia and mood disturbances. Deletion of xCT in the tumor strongly reduced tumor growth. Targeting xCT in the host and not the tumor resulted only in a partial reduction of tumor burden, while it did attenuate tumor-related systemic inflammation and prevented an increase in immunosuppressive regulatory T cells. The latter effect could be replicated by specific xCT deletion in immune cells. xCT deletion in the host or the tumor differentially modulated neuroinflammation. When mice were grafted with xCT-deleted tumor cells, hypothalamic inflammation was reduced and, accordingly, food intake improved. Tumor bearing $xCT^{-/-}$ mice showed a trend of reduced hippocampal neuroinflammation with less anxiety- and depressive-like behavior.

Taken together, targeting xCT may have beneficial effects on pancreatic cancer-related comorbidities, beyond reducing tumor burden. The search for novel and specific xCT inhibitors is warranted as they may represent a holistic therapy in pancreatic cancer.

1. Introduction

Pancreatic ductal adenocarcinoma (PDAC) is one of the most malignant cancers with a five-year survival rate of only 10 % (Mizrahi et al., 2020) and pancreatic cancer mortality is predicted to double by the year 2060, according to WHO projections (Lippi and Mattiuzzi, 2020). These numbers can be attributed to an aggressive tumor and treatment resistance, as well as an immunosuppressive tumor microenvironment

* Corresponding authors at: Laboratory of Neuro-Aging & Viro-Immunotherapy, Vrije Universiteit Brussel, Laarbeeklaan 103, 1090 Brussels, Belgium (A. Massie), Laboratory for Medical and Molecular Oncology, Vrije Universiteit Brussel, Laarbeeklaan 103, 1090 Brussels (I. Rooman).
E-mail addresses: ilse.rooman@vub.be (I. Rooman), ann.massie@vub.be (A. Massie).
[1] Equally contributing first authors.
[2] Equally contributing senior authors.

https://doi.org/10.1016/j.bbi.2024.03.001
Received 7 July 2023; Received in revised form 5 February 2024; Accepted 2 March 2024
Available online 4 March 2024
0889-1591/© 2024 The Authors. Published by Elsevier Inc. This is an open access article under the CC BY license (http://creativecommons.org/licenses/by/4.0/).

characterized by the presence of regulatory T (Treg) cells, myeloid-derived suppressor cells (MDSC) and tumor-associated macrophages (Kleeff et al., 2016; Connor and Gallinger, 2022). Yet, pancreatic cancer-related comorbidities also contribute to the poor patient survival. Cachexia, a multisystemic syndrome causing anorexia and muscle catabolism, occurs in approximately 80 % of pancreatic cancer patients and is considered a major cause of PDAC mortality (Poulia et al., 2020). Furthermore, it is hypothesized that a bidirectional link between cancer and the central nervous system exists, that induces psychiatric comorbidities such as depression and anxiety, thereby further reducing the quality-of-life of cancer patients (Santos and Pyter, 2018). In pancreatic cancer patients, depression and anxiety were diagnosed more frequently in the year preceding cancer diagnosis compared to a control population, suggesting that in addition to the psychological stress that comes with cancer diagnosis, tumor-intrinsic factors are important root causes for cancer-induced mood disturbances (Davis et al., 2022).

Systemic and central inflammation are important drivers of both cachexia and depression (Santos and Pyter, 2018; Tan et al., 2014; Zimmers et al., 2016; Dantzer, 2006; Lee and Giuliani, 2019). Tumor cells as well as non-tumor cells in the tumor microenvironment secrete inflammatory cytokines that can reach the brain and induce neuroinflammation (Santos and Pyter, 2018). The hypothalamus in particular, was shown to be a critical brain region in cachexia (Michaelis et al., 2017; Grossberg et al., 2010).

The cystine/glutamate antiporter system x_c^-, with its specific subunit xCT, exchanges extracellular cystine for intracellular glutamate at a 1:1 ratio. The imported cystine is reduced intracellularly to cysteine, a building block of the antioxidant glutathione (GSH), thereby protecting cells against oxidative stress. Cancer cells upregulate xCT to promote their survival and drug resistance (for review (Lo et al., 2008)), and xCT expression is increased by chemotherapy as such further contributing to the resistance mechanism (Starheim et al., 2016; Wang et al., 2016; Zhang et al., 2016). Several strategies to target xCT in cancer have been explored. Although not being specific, the best studied approach -besides genetic modulation- is the use of sulfasalazine (SAS), an FDA-approved anti-inflammatory drug that also inhibits system x_c^-. Treatment with SAS was shown to induce a chemo-sensitizing effect in different cancer types and to cause tumor cell death (for review (Lo et al., 2008)).

In physiological conditions, xCT is mainly expressed in the central nervous system and in the immune system (Lewerenz et al., 2013; Massie et al., 2015). As an important source of extracellular glutamate in several brain regions (De Bundel et al., 2011; Massie et al., 2011), system x_c^- modulates glutamate-sensitive behavior in mice. Genetic deletion of xCT results in anxiolytic and anti-depressive-like effects both in physiological (Bentea et al., 2015) and pathological conditions. Pharmacological or genetic targeting of system x_c^- reduces depressive-like behavior in a breast cancer model (Nashed et al., 2017) and in LPS-challenged mice (Albertini et al., 2018), respectively. In the latter study, these behavioral effects were accompanied by a more efficient resolution of peripheral inflammation that resulted in reduced LPS-induced neuroinflammation in xCT-deficient mice. The function of system x_c^- on cells of the peripheral immune system is, however, poorly understood. It is generally accepted that xCT is expressed on cells of the innate immune system (Lewerenz et al., 2013) and activated T cells (Siska et al., 2016; Levring et al., 2012), but not on naive lymphocytes (Srivastava et al., 2010; Angelini et al., 2002).

Targeting xCT beyond the tumor, could thus have beneficial effects in cancer by impacting on the comorbidities. We therefore investigated the effect of xCT deletion on the tumor, the immune cells and/or the entire host, with a focus on inflammation, cachexia and mood disturbances. While most studies focused on targeting xCT in the tumor, we here provide additional evidence that inhibition of system x_c^- outside of the pancreatic tumor reduces systemic inflammation and neuroinflammation, highlighting it as a therapeutic angle to diminish the comorbidities of pancreatic cancer.

2. Materials and methods

2.1. Cell lines and culture

Panc02 cells (gift from Dr. C. Gravekamp, Albert Einstein College of Medicine, New York, USA (Chandra et al., 2017)) and KPC cells (gift from Dr. E. Jaffee, Johns Hopkins University, Baltimore, USA (Foley et al., 2015)) were maintained in supplemented culture medium (RPMI 1640 + L-glutamine, supplemented with 10 % Fetal Bovine Serum, 1 % Penicillin/Streptomycin, 1 % Sodium Pyruvate and 1 % Minimum Essential Medium Non-Essential Amino Acids; all from Thermo Fisher Scientific), in a humidified atmosphere at 37 °C and 5 % CO_2. All cell lines were routinely tested for mycoplasma throughout the study.

2.2. CRISPR/Cas9-mediated xCT knockout Panc02 and KPC cells

xCT deletion was induced in Panc02 (Panc02 KO) and KPC (KPC KO) cells by CRISPR/Cas9-mediated genome editing, using the LentiCRISPRv2-puro vector (Addgene plasmid #98290). Guide RNAs (gRNA) were designed using the MIT CRISPR tool and the gRNA with the least predictive off-target activity was selected. Oligonucleotides targeting xCT (5′ CACCGGGGCTACGTACTGACAAACG 3′) were cloned in the LentiCRISPRv2-puro vector, according to the manufacturer's instructions (Addgene) and followed by third generation lentiviral production. To prepare lentivirus, HEK 293 T cells were transfected using polyethyleneimine transfection reagent (Sigma-Aldrich) with the packaging plasmids REV (6.25 μg) and GAG (12.5 μg), the envelope plasmid VSV-G (9 μg) and the transgene encoding plasmid (37.5 μg). Lentiviral supernatants were harvested 48 and 72 h after transfection. Panc02 and KPC cells were seeded in a 6-well plate at a density of 100.000 cells/well and transduced with lentiviral supernatants supplemented with 10 μg/mL protamine sulphate and 50 μM 2-mercaptoethanol (2-ME) (both from Sigma-Aldrich) for 24 h. After one week, transduced cells were selected with 7 μg/mL puromycine (Merck) for Panc02 cells and 6 μg/mL for KPC cells, until all non-transduced cells died.

2.3. Analysis of xCT mRNA expression in human PDAC samples

RNA expression data of sorted human PDAC were obtained from a previously published dataset (Espinet et al., 2021). PDAC specimens originated from patients who received partial pancreatoduodenectomy at the Department of General, Visceral and Transplantation Surgery, University of Heidelberg. Patients were part of the HIPO-project. The study was approved by the ethical committee of the University of Heidelberg (case number S-206/2011 and EPZ-Biobank Ethic Vote #301/2001) and conducted in accordance with the Helsinki Declaration; written informed consent was obtained from all participating patients.

2.4. Cell proliferation and viability assay

Panc02 (5.000 cells/well) and KPC (4.000 cells/well) wildtype (WT) and KO cells were seeded in supplemented culture medium in the presence or absence of 50 μM 2-ME in a flat bottom 96-well plate. Cell proliferation was assessed using the IncuCyte® Live-Cell Analysis System (Essen Bioscience) for 48 h with phase contrast image acquisition every 2 h. Analysis of cell surface confluency was performed using the IncuCyte ZOOM software (Essen Bioscience, GUI Version 2018A). Cell viability was determined using the CellTiter-Glo® Luminescent Assay (Promega) following manufacturer's instructions, at the end of cell proliferation assessment.

2.5. [^{3}H]-L-Glutamate uptake assay

System x_c^- - activity was quantified by measuring the reversed uptake of [^{3}H]-L-glutamate, and specificity of the assay was confirmed as described before (Beckers et al., 2022).

2.6. Animal experimentation

Male mice with a genetic deletion of xCT ($xCT^{-/-}$) and their wildtype ($xCT^{+/+}$) littermates are high-generation descendants of the strain originally described by Sato *et al.* (Sato et al., 2005) and have a C57BL/6J background. All mice were bred in a heterozygous colony at the Vrije Universiteit Brussel. Genotyping of the mice was performed as described before (Massie et al., 2011). Eight to ten weeks old Ly5.1 male mice (C57BL/6J background) were used as recipients for transplantation with bone marrow (BM) originating from $xCT^{+/+}$ or $xCT^{-/-}$ mice.

Mice were single-housed under standardized conditions (20–24 °C, 10/14 h dark/light cycle, 45–65 % humidity) with water and food *ad libitum*. All experiments were approved by the Ethical Committee for Animal Experimentation of the Vrije Universiteit Brussel and performed according to the European guidelines on animal experimentation. All efforts were made to minimize animal suffering.

2.7. Bone marrow transplantation

Bone marrow transplantations (BMT) were performed as described before (Janssen et al., 2023). Ly5.1 mice were sublethally irradiated at a split dose of 11 Gy (2x5.50 Gy) with a TrueBeam® system (Varian Medical System) at 4 h interval. Six to eight hours after the second irradiation session, irradiated mice received an intravenous injection (in the tail vein) of $10x10^6$ BM cells, freshly collected from $xCT^{+/+}$ and $xCT^{-/-}$ mice by flushing the tibiae and femur cavities with Hank's Balanced Salt Solution (HBSS, Lonza) supplemented with 2 % Fetal Bovine Serum (Thermo Fisher Scientific). Mice received 0.01 % Enrofloxacin (Sigma-Aldrich) in their drinking water for one month following the BMT procedure. Chimerism was confirmed (91.6 ± 3.1 % replacement) on a blood sample, collected eight weeks after BMT (i.e. one week before injection of the tumor cells), based on the CD45.1 isoform expression on immune cells in Ly5.1 mice versus CD45.2 expression in xCT transgenic mice, using flow cytometry. Blood cells were stained with fixable viability stain-780 (diluted 1/4000 in phosphate-buffered saline (PBS), Thermo Fisher Scientific), followed by staining with antibodies against CD45.1 and CD45.2 (Supplementary Table S1). Samples were analyzed with a BD LSR Fortessa flow cytometer (BD Biosciences).

2.8. Experimental design

Mice were 3–4 months old at the start of the experiment. $5x10^6$ Panc02 WT or KO tumor cells resuspended in PBS were injected intraperitoneally (i.p.) in the left iliac region, while control mice received an injection with PBS. Seven days before tumor cell engraftment, mice were single-housed, and assessment of food intake and body weight was started on a daily basis. Sifting of the bedding was performed to collect spilled food that was taken into account in the daily food intake. Cachexia was defined as the interval starting with two consecutive days with a > 10 % decrease in average food intake (Michaelis et al., 2017). Spontaneous locomotion and anxiety-like behavior were assessed using the open field test at day 8 *post* tumor cell engraftment, and depressive-like behavior at day 9 and 10 using the tail suspension test and forced swim test. At day 14 after inoculation with tumor cells, mice were sacrificed, and the tumor was dissected and weighed. Blood and ascites were collected, and ascites was scored as described before (Chandra et al., 2017). Spleen, brain, heart and gastrocnemius muscle were dissected and processed for further analysis.

2.9. Quantitative reverse transcription-polymerase chain reaction (qRT-PCR)

Total RNA was isolated from Panc02 and KPC cells with the NucleoSpin RNA isolation kit (Macherey-Nagel), from hippocampal and hypothalamic tissue with the RNeasy Lipid Tissue Mini Kit (Qiagen) and from gastrocnemius muscle tissue with the RNeasy Mini Kit (Qiagen). RNA concentration was determined using the NanoDrop2000 (Thermo Fisher Scientific), and followed by reverse transcription using the Qscript cDNA synthesis kit (Quantabio). Real-time PCR on cDNA of pancreatic cancer cells was performed using FastSYBRGreen 5X Master Mix (Thermo Fisher Scientific), and on cDNA of brain and muscle tissue as described before (Verbruggen et al., 2022), using the primers in Supplementary Table S2. Analysis of the data was performed with the $2^{-\Delta\Delta Ct}$ method, using Ywhaz as housekeeping gene for brain and muscle tissue, and HPRT for pancreatic cancer cells.

2.10. Flow cytometry

Splenocytes were collected by gently homogenizing the spleen through a cell strainer (40 μm nylon, CORNING Life Sciences), followed by removal of erythrocytes using red blood cell lysis buffer (150 mM NH_4Cl, 10 mM $KHCO_3$ and 0.13 mM EDTA; pH 7.2; Sigma-Aldrich). Splenocytes were stored in liquid nitrogen in cryopreservation medium that is specifically developed for sensitive cell types (Cryostor® CS10, Stemcell Technologies), until further analysis. $2x10^6$ cells (or $4x10^6$ cells for the assessment of Tregs) were stained with fixable viability stain-780 (1/4000 in PBS) for 20 min in the dark at room temperature, followed by staining with antibodies against cell surface markers for T cells, NK cells and various myeloid cell populations (Supplementary Table S1). Intracellular Foxp3 staining was performed after fixation and permeabilization of the cells with eBioscience Foxp3/Transcription Factor Staining Buffer Set (Invitrogen). Cells were analyzed using a BD LSR Fortessa cytometer. All read-outs had control samples of matching cells that were unstained to rule out autofluorescence and fluorescence minus one controls were used for set-up. Data were analyzed using Flowlogic software (Miltenyi Biotech); the gating strategy is shown in Supplementary Fig. S1.

2.11. Plasma cytokine assessment

Plasma levels of cytokines were analyzed in undiluted samples using a U-PLEX Custom Biomarker group 1 mouse assay (K15069M-1; multiplexed: IL-1β, TNF-α, IL-6, IL-10 and IFN-γ) and MSD QuickPlex SQ120MM instrument (Meso Scale Diagnostics), according to the manufacturer's instructions. Values below the detection limit were replaced by a value calculated by the lower limit of detection for that cytokine divided by square root of 2.

2.12. Western blotting

Total protein lysates were obtained by homogenizing pancreatic cancer cells with RIPA buffer (100 mM Tris pH 7.4, 150 mM NaCl, 1 mM EDTA, 1 % Triton X-100, 0.1 % sodium dodecyl sulphate, 1 % sodium deoxycholate; Sigma-Aldrich). Hypothalamic and hippocampal tissue was processed, and xCT protein levels quantified as described before (Albertini et al., 2018; Van Liefferinge et al., 2016) using the antibodies specified in Supplementary Table S1. xCT expression levels were determined relative to a pooled sample and normalized to a total protein stain. $xCT^{-/-}$ hypothalamic or hippocampal samples, or KO cell lysates were included in each experiment as a negative control.

2.13. Behavioral analyses

Behavioral tests were performed as described before, with minor modifications (Albertini et al., 2018; Bentea et al., 2015), and video-recorded by a researcher blinded to the experimental groups. An automated integration system (Ethovision software, Noldus) was used to analyze the open field test; analysis of the other tests was done by a blinded researcher. Anxiety-like behavior was assessed by placing mice in an open field (60 cm x 60 cm x 60 cm) with its center illuminated by 130 lx, for 15 min. Spontaneous locomotor activity of the mice was

measured, with the percentage of time spent in the center of the open field, defined as the central 40 x 40 cm zone, as an indicator for anxiety-like behavior. Depressive-like behavior was studied by suspending mice by the extremity of their tail (i.e. tail suspension test) and by placing mice in a glass tank filled with 30 cm of water (25 °C ± 1 °C) (i.e. forced swim test) for 5 min in a set-up that was brightly illuminated by 350 lx. Immobility time or counts (Bentea et al., 2015) were quantified as a measure for depressive-like behavior. Mice that climbed their tail during the tail suspension test were excluded from the analysis. Finally, general wellbeing and fine sensorimotor function were assessed using the nest building test, as described before (Deacon, 2006). The evening before the test, all enrichment in the cage was removed except one pressed cotton to build a nest. The following morning, the nest was scored (1 = absence of a nest and 5 = perfect nest) and the weight of the unused nesting material was recorded.

2.14. Statistical analysis

Data are presented as mean ± standard error of the mean (SEM). Statistical analyses were performed using unpaired two-tailed *t*-test, one- or two-way (mixed-model) ANOVA with Tukey's or Sidak's post hoc tests or Chi-square test, with the GraphPad Prism 9 software.

For the peripheral and central cytokine levels, additional analyses were performed in SPSS and R by configuring the most optimal statistical model that takes the tumor mass into account as a covariate. A multi-way ANCOVA model was configured by means of a sequential forward elimination. For each dependent variable of interest, the following independent variables are considered including their possible two-way and three-way interactions: tumor weight, $xCT^{+/+}$ versus $xCT^{-/-}$ mice, and Panc02 WT versus KO groups. The optimal model configuration that maximized the adjusted R^2 value was retained. Variables that are not retained by the model, are deemed insignificant. If tumor weight is not picked up as a confounder, the initial two-way ANOVA remains the most appropriate model.

For all analyses, the α-value was set at 0.05. Significant outliers were removed from the dataset, after identification by the Grubb's outlier test (α-value = 0.05). The normality of the residuals was evaluated using the D'Agostino and Pearson omnibus normality test, and the Brown-Forsythe test was used to test for equal variances. Upon violations of equal variances, no correction was performed. We recognize that in the presence of unequal variances the tests applied suffer from a loss in statistical power. However, in case the data were not normally distributed, we performed a transformation before applying the statistical test. A correction for departures from normality is needed to ensure that all p-values rendered are correct and hence trustworthy conclusions can be drawn. Graphs with the non-transformed data are shown for all experiments for the ease of interpretation of the data. In case no transformation could be found to obtain a normal distribution, we performed a non-parametric one-way or two-way ANOVA on the untransformed data. All details on statistical analyses, as well as outlier detection, are given in Supplementary Table S3.

3. Results

3.1. xCT deletion in pancreatic tumor cells reduces in vitro proliferation and in vivo tumor growth

In humans, PDAC is among the highest xCT (SLC7A11) expressing cancers (Supplementary Fig. S2A), with the strongest xCT mRNA expression in tumor epithelial cells and notable heterogeneity in expression levels (Fig. 1A) (Espinet et al., 2021). Indeed, the two murine PDAC cell lines we used in this study had profound differences in both xCT expression (Fig. 1B) and activity (Fig. 1C). To assess the function of xCT in these cells, we deleted xCT in the Panc02 (Panc02 KO) and KPC (KPC KO) mouse cell lines using CRISPR/Cas9-mediated genome editing. Reduced xCT mRNA (Supplementary Fig. S2B and C) and protein expression (Supplementary Fig. S2D and E) resulted in significantly lowered system x_c^- - activity as evidenced by a decrease in [^{3}H]-L-glutamate uptake in both cell lines (Fig. 1C). Targeting xCT also induced a significant decrease in intracellular GSH levels in Panc02 KO and KPC KO cells, compared to WT cells, that could be (partly) rescued by addition of 2-ME to the culture medium (Fig. 1D and G), as such bypassing system x_c^- for cysteine transport in the cell (Lewerenz et al., 2013). We next measured tumor cell proliferation *in vitro* and showed that loss of xCT renders both Panc02 and KPC cells unable to proliferate in the absence of 2-ME (Fig. 1E and H). Similarly, 48 h after seeding, cell viability was decreased in the xCT KO cells compared to WT cells and was rescued by 2-ME (Fig. 1F and I).

Given the higher system x_c^- activity in Panc02 compared to KPC cells (Fig. 1C), we continued with this cell line for *in vivo* experiments. Panc02 WT and Panc02 KO cells were i.p. injected in $xCT^{+/+}$ mice. In line with our *in vitro* results, we observed significantly reduced tumor growth (Fig. 1J) and a trend towards attenuated ascites production (Fig. 1K) 14 days after injecting Panc02 KO cells in $xCT^{+/+}$ mice when comparing to WT cells. Likewise, we only observed an endpoint increase in body weight in the $xCT^{+/+}$ mice injected with Panc02 WT -and not with Panc02 KO- cells compared to PBS control mice (Fig. 1L). Of note, these findings could not be reproduced by treatment of C57BL/6J mice injected with Panc02 WT tumors with SAS, the best available option to pharmacologically inhibit xCT (Supplementary methods and Supplementary Fig. S3A–C).

Besides being highly upregulated on tumor cells, we also detected xCT on cells of the stroma, including the immune stroma (Fig. 1A). Moreover, its expression in the peripheral immune system was reported before (Lewerenz et al., 2013). Targeting xCT in the entire host (or exclusively on immune cells, see further), might thus influence tumor burden and tumor-induced inflammation. Therefore, to dissect the role of tumor xCT versus host xCT, we first injected Panc02 WT and Panc02 KO cells in full body $xCT^{-/-}$ mice. A significant reduction in tumor weight and trend for reduced ascites formation were still observed when targeting xCT both in the tumor and host, while deletion of xCT exclusively in the host only resulted in a partial, non-significant reduction in tumor burden ($p = 0.2210$) (Fig. 1J and K).

3.2. Host xCT deletion attenuates peripheral inflammation and Treg immunosuppressive cells

In a next step, we assessed the effect of xCT deletion on tumor-induced peripheral inflammation in PDAC mice. All inflammatory cytokine levels significantly increased in the presence of a tumor, except for IL-1β (Fig. 2A–E). The tumor induced a strong increase in plasma IL-6 levels, that was reduced upon tumor xCT deletion as well as in $xCT^{-/-}$ mice grafted with either Panc02 WT or KO cells (Fig. 2B**)**. Moreover, engraftment with Panc02 WT cells induced a significant increase in IFN-γ levels in both $xCT^{+/+}$ and $xCT^{-/-}$ mice, while this increase was not observed in mice with Panc02 KO tumors (Fig. 2C). The tumor-induced increase in TNF-α levels was the most pronounced in $xCT^{+/+}$ mice (Fig. 2D). Interestingly, the increase in anti-inflammatory IL-10 levels was most significant in $xCT^{-/-}$ mice (Fig. 2E). A more profound statistical analysis including tumor size as a covariate (ANCOVA, Supplementary Fig. S4) revealed whether these observed changes in cytokine levels were the direct effect of differences we observed in tumor weight (Fig. 1J). IL-1β, IL-6, IFN-γ and TNF-α levels mainly depended on tumor weight (Supplementary Fig. S4A–D). However, for IL-10, the presence -and not the size- of the tumor was the most important determinant factor, and resulted in an overall tumor-induced increase in IL-10 concentrations (Supplementary Fig. S4E).

Besides peripheral cytokines, we also assessed the different populations of immune cells in the spleen. No tumor- or mouse genotype-related changes were detected in the proportion of $CD8^+$ or $CD4^+$ T cells in the spleen (Supplementary Fig. S5A–K). However, host xCT deletion did prevent the tumor-induced increase in Treg cells that is

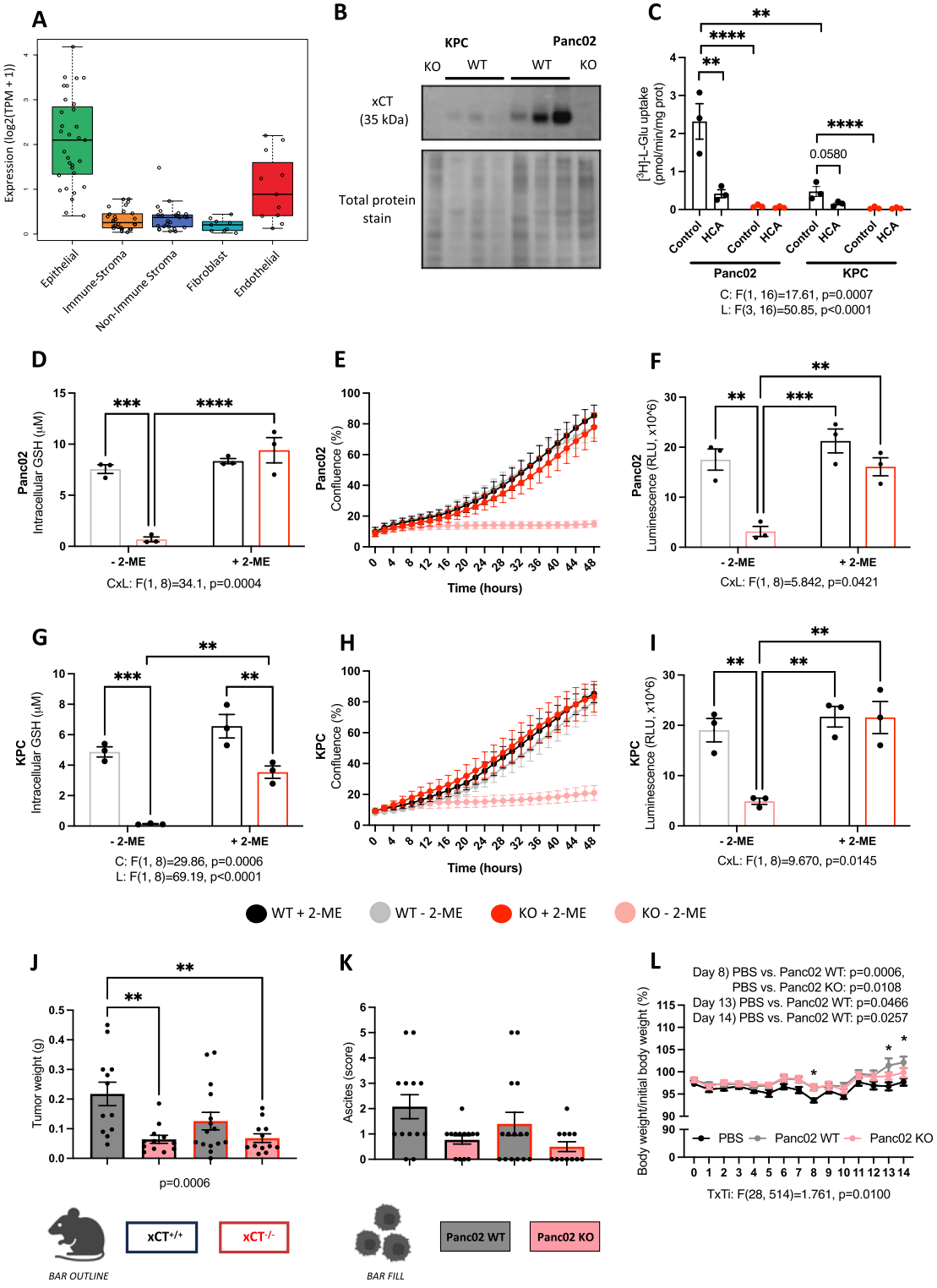

Fig. 1. Pancreatic cancer cells rely on xCT expression for *in vitro* and *in vivo* proliferation. A) xCT mRNA expression levels (transcript per million, TPM + 1) in purified epithelial cells, stroma, fibroblasts and endothelial cells from human PDAC samples. B) Western blot illustrating protein expression of xCT in Panc02 and KPC WT cells. C) Activity of system x_c^- assessed by measuring [^{3}H]-L-glutamate uptake in xCT WT and KO cells under control conditions and after addition of the system x_c^- inhibitor HCA. D,G) Intracellular GSH levels 24 h after cell seeding and normalized to CellTiterGlo®. E,H) Incucyte percentage of confluency (n = 3) and F, I) cell viability at 48 h by CellTiterGlo®. J) Tumor weight and K) ascites score of xCT$^{+/+}$ and xCT$^{-/-}$ mice grafted with Panc02 WT or Panc02 KO cells (n = 13–15 mice/group). L) Body weight of the xCT$^{+/+}$ mice relative to their initial body weight over the course of the experiment. Data are presented as mean ± SEM, and analyzed using a two-way ANOVA, followed by Tukey's or Sidak's multiple comparisons test (C,D,F,G,I), a one-way ANOVA followed by Tukey's multiple comparisons test (J,K) or a two-way ANOVA mixed-model, followed by Tukey's multiple comparisons test (L). Significant main effects are indicated below the graph: C condition effect, L cell line effect, CxL interaction effect, TxTi interaction effect between tumor (genotype) (T) and time (Ti). + 2-ME indicates the addition of 50 μM 2-ME. *p < 0.05, **p < 0.01, ***p < 0.001, ****p < 0.0001, 2-ME 2-mercaptoethanol, HCA homocysteic acid, GSH gluthatione, RLU relative light unit.

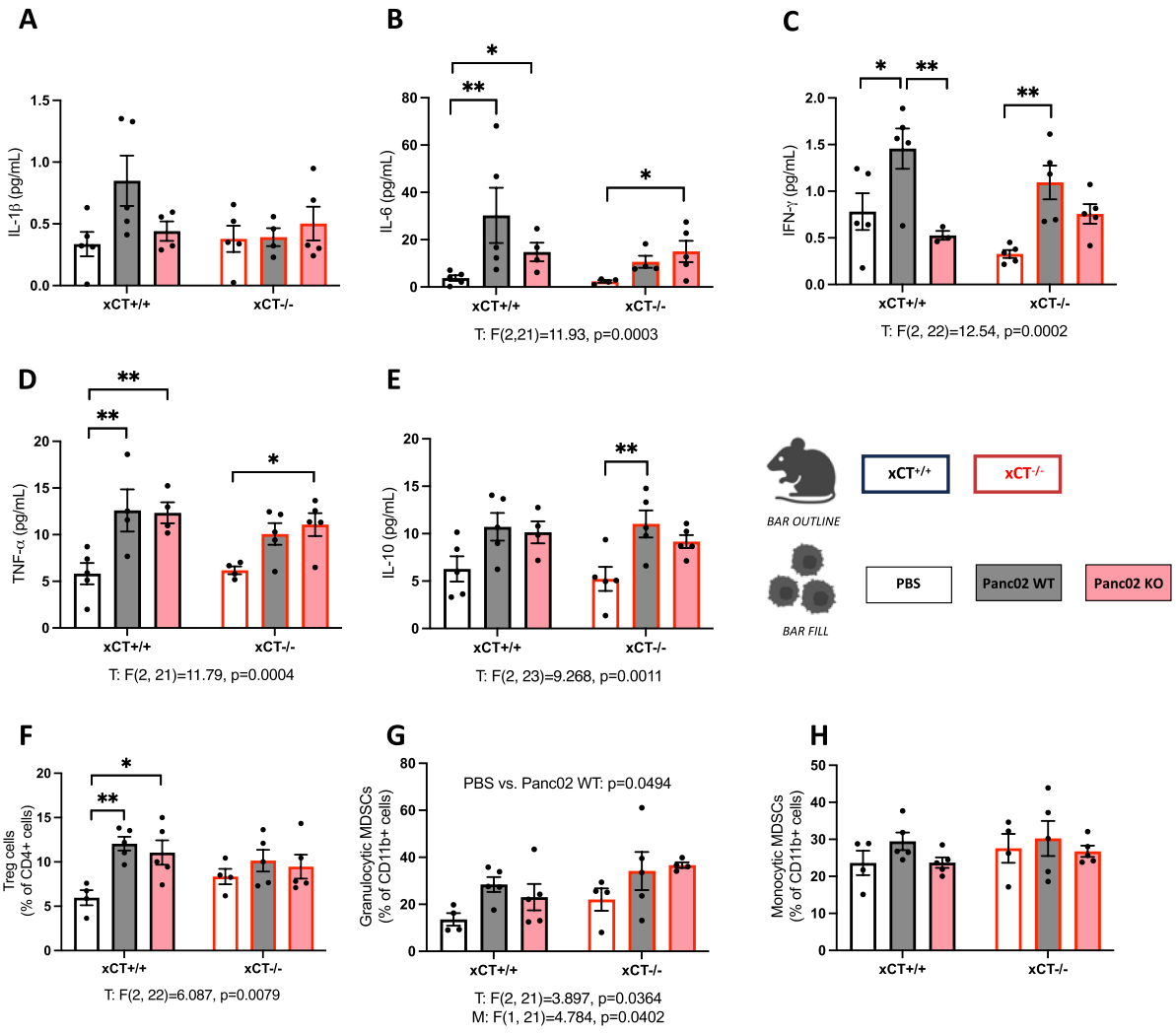

Fig. 2. Host xCT deletion attenuates peripheral inflammation and the tumor-induced increase in Treg population. $xCT^{+/+}$ and $xCT^{-/-}$ mice were injected i.p. with PBS, Panc02 WT or Panc02 KO cells. A-E) Plasma cytokine concentrations of IL-1β (A), IL-6 (B), IFN-γ (C), TNF-α (D) and IL-10 (E) (n = 3–5 mice/group). F-H) Fraction of Treg cells (F), granulocytic MDSCs (G) and monocytic MDSCs (H) from the total living single-cell splenocyte population (n = 4–5 mice/group). Gating strategy for the different subpopulations is shown in Supplementary Fig. S1. Data are presented as mean ± SEM and were analyzed by a two-way ANOVA followed by a Tukey's or Sidak's multiple comparisons test. Significant main effects of the two-way ANOVA are indicated below the graph: T tumor (genotype) effect, M mouse genotype effect. Significant simple effects of the multiple comparisons test are indicated on the bars: *p < 0.05, **p < 0.01. In the absence of significant simple effects, the significant main group effects of the multiple comparisons test are indicated above the graph. Treg regulatory T cell, MDSC myeloid-derived suppressor cell.

clearly observed in $xCT^{+/+}$ mice grafted with either Panc02 WT or KO cells (Fig. 2F). We also measured a significant increase in granulocytic MDSCs -an overall tumor effect driven by WT tumor that could not be prevented by host xCT deletion- (Fig. 2G) without changing the proportion of monocytic MDSCs (Fig. 2H). Albeit we detected some overall mouse genotype effects that were not affected by the genotype of the tumor, we did not observe major changes in the innate immune cell population (Supplementary Fig. S5L–P) or the weight of the spleen (Supplementary Fig. S5Q).

Next we investigated whether any of these effects could be reproduced by solely deleting xCT in the immune cells, using BM chimeras. This did however not impact tumor weight or ascites (Fig. 3A and B), neither peripheral inflammation (Fig. 3C–G) nor the proportion of $CD8^+$ or $CD4^+$ T cells (Fig. 3H and I), while the attenuating effect on the tumor-induced increase in Tregs that we observed in $xCT^{-/-}$ mice (Fig. 2F) is maintained in the $xCT^{-/-}$ BM grafted mice (Fig. 3J). The proportion of MDSCs was not altered by specific immune xCT deletion (Fig. 3K and L).

Altogether, our results show that both tumor and host xCT deletion -either directly or indirectly by reducing tumor size- attenuated peripheral inflammation. Yet, only host or immune cell -and not tumor- xCT deletion reduced the tumor-induced immunosuppressive Treg cell population.

3.3. *Tumor xCT deletion attenuates hypothalamic inflammation and early signs of muscle wasting, and improves food intake*

Since it was reported that inflammatory mediators can diffuse to the brain (Santos and Pyter, 2018), and our results indicate that both deletion of host xCT or tumor xCT reduce tumor-related peripheral inflammation (Fig. 2A–E), we next studied whether this also attenuates neuroinflammation in our PDAC model. We first focused on hypothalamic inflammation, which is a feature of cachexia (Grossberg et al., 2010). Tumor xCT deletion significantly reduced IL-6 (Fig. 4A) and TNF-α (Fig. 4B) mRNA levels in the hypothalamus, without affecting IL-1β mRNA (although a similar trend is observed; Fig. 4C). Similar to the peripheral inflammation, we evaluated if the reduced hypothalamic inflammation could be attributed to lower KO tumor weight. Yet, the

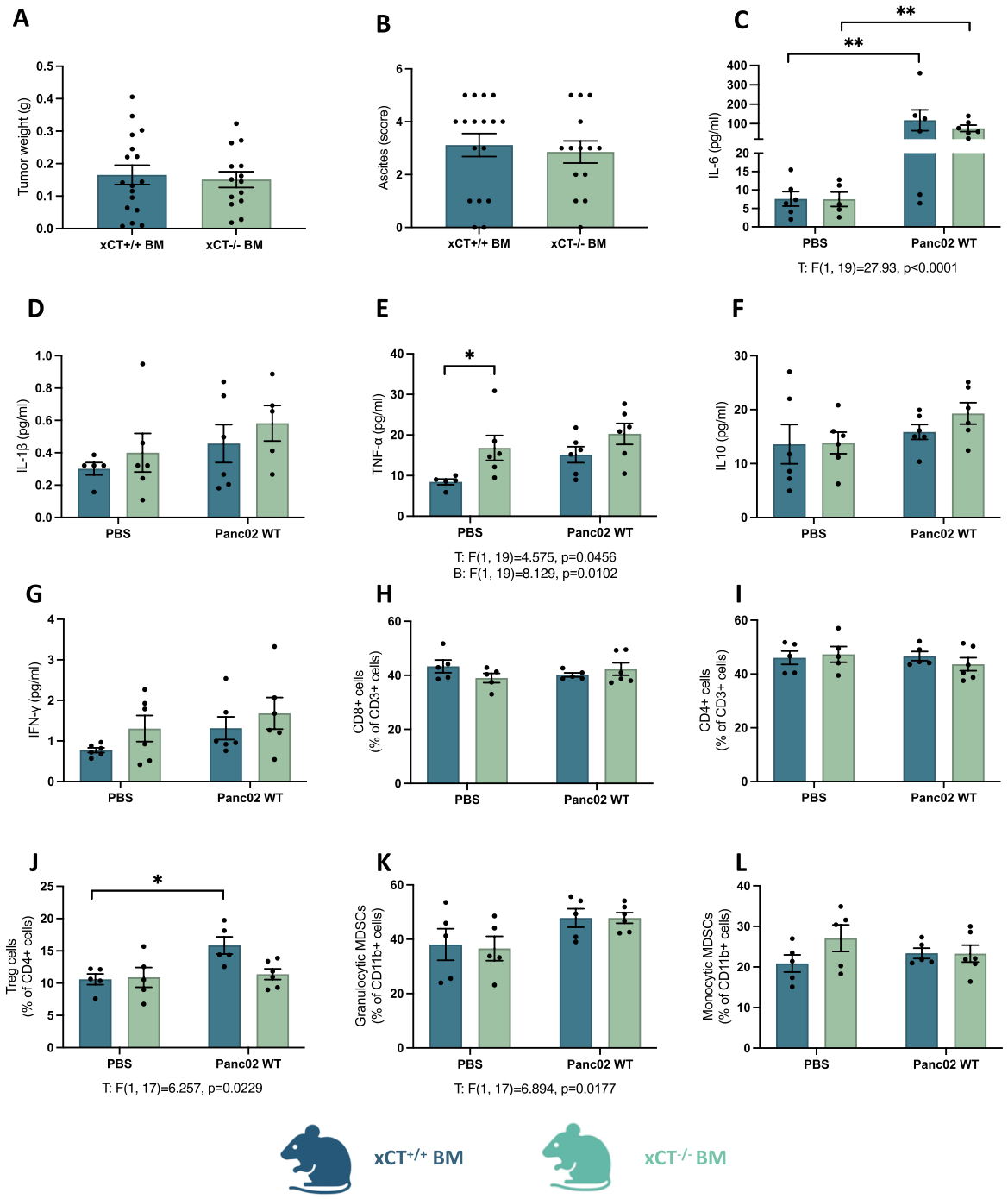

Fig. 3. Specific targeting of xCT on immune cells has no effect on peripheral inflammation or tumor burden, but reduces the Treg population. A) Tumor weight and B) ascites score of $xCT^{+/+}$ and $xCT^{-/-}$ BM mice grafted i.p. with Panc02 WT cells (n = 14–17 mice/group). C-G) Plasma cytokine levels of IL-6 (C), IL-1β (D), TNF-α (E), IL-10 (F) and IFN-γ (G) (n = 6 mice/group). H-L) Fraction of $CD8^+$ T cells (H), $CD4^+$ T cells (I), Treg cells (J), granulocytic MDSCs (K) and monocytic MDSCs (L) from the total living single-cell splenocyte population (n = 5–6 mice/group). Gating strategy for the different subpopulations is shown in Supplementary Fig. S1. Data are presented as mean ± SEM and were analyzed by an unpaired two-tailed *t*-test (A,B) or a two-way ANOVA followed by Sidak's multiple comparisons test (C-L). Significant main effects of the two-way ANOVA are indicated below the graph: T tumor effect, B BM effect. Significant simple effects of the multiple comparisons test are indicated on the bars: *p < 0.05, **p < 0.01, Treg regulatory T cell, MDSC myeloid-derived suppressor cell.

weight of the tumor only correlated with IL-1β, and not IL-6 or TNF-α mRNA levels in the brain (Supplementary Fig. S6A where only cytokines that significantly correlate with tumor size are shown), indicating that the observed reduction in inflammatory cytokines is not merely a consequence of reduced tumor size and absence of xCT brings additional benefit. Hypothalamic xCT protein expression -that is known to be increased by inflammatory stimuli (Albertini et al., 2018; Lewerenz et al., 2013; Massie et al., 2015)- is unaffected after grafting $xCT^{+/+}$ mice with Panc02 WT or KO tumors (Fig. 4D).

Attenuated hypothalamic inflammation was in line with improved food intake, which is reduced in -and one of the important hallmarks of- cachexia (Grossberg et al., 2010). Although tumor xCT deletion did not majorly affect the proportion of mice suffering from cachexia (41 % for Panc02 KO tumors vs. 52 % for Panc02 WT tumors) (Fig. 4E), endpoint

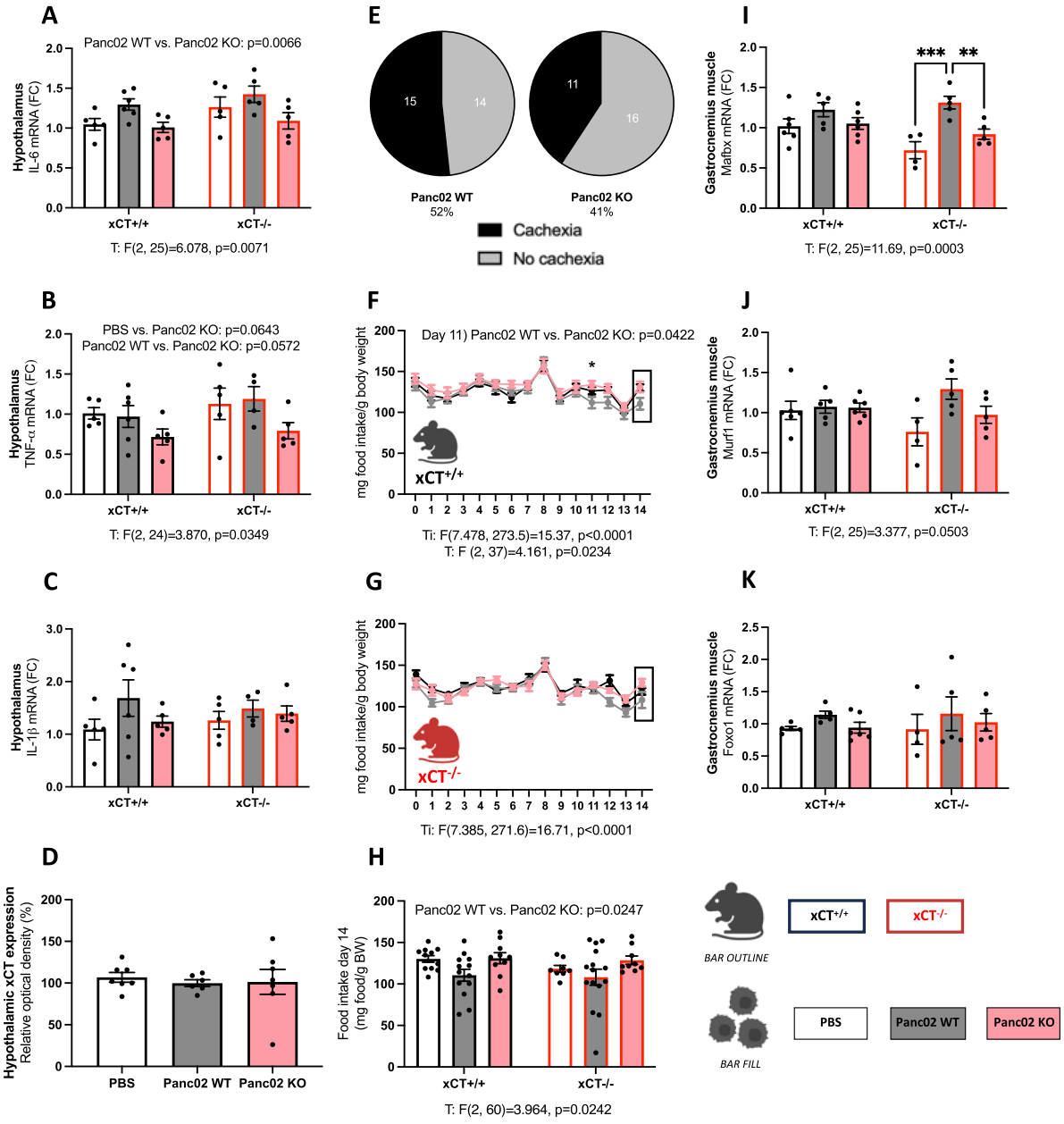

Fig. 4. Deletion of xCT in the tumor cells reduces hypothalamic inflammation and skeletal muscle catabolism, and increases food intake. $xCT^{+/+}$ and $xCT^{-/-}$ mice were injected i.p. with PBS, Panc02 WT or Panc02 KO cells. A-C) Hypothalamic IL-6 (A), TNF-α (B) and IL-1β (C) mRNA levels (n = 5–6 mice/group). Results are expressed as fold change (FC), relative to $xCT^{+/+}$ control mice. D) xCT protein expression levels in $xCT^{+/+}$ mice (n = 6–7 mice/group; three independent experiments were performed, of which one representative experiment is shown). E) Proportion of mice suffering from cachexia induced by a xCT WT or KO tumor. F-G) Food intake, relative to body weight, over the course of the experiment and H) at day 14. I-K) Mafbx (I), Murf1 (J) and Foxo1 (K) mRNA levels in the gastrocnemius muscle (n = 4–6 mice/group). Results are expressed as FC, relative to $xCT^{+/+}$ control mice. Data are presented as mean ± SEM and were analyzed using a non-parametric one-way ANOVA (D), a two-way ANOVA followed by Tukey's or Sidak's multiple comparisons test (A-C,H-K), a two-way ANOVA mixed-model (F,G) or a Chi-square test (E). Significant main effects of the two-way ANOVA are indicated below the graph: T tumor (genotype) effect, Ti time effect. Significant simple effects of the multiple comparisons test are indicated on the bars: *p < 0.05, **p < 0.01, ***p < 0.001. In the absence of significant simple effects, the significant main group effects of the multiple comparisons test are indicated above the graph.

food intake in mice with tumor xCT deletion was increased compared to mice with xCT expressing tumors and could not be distinguished from PBS control mice (Fig. 4F–H).

While no significant changes were seen in the weight of the gastrocnemius muscle (Supplementary Fig. S7A) or cardiac mass (Supplementary Fig. S7B), we also assessed the expression of E3 ubiquitin ligase-related genes that are associated with skeletal muscle catabolism (Michaelis et al., 2017). The expression of the gene Mafbx was significantly increased in the gastrocnemius muscle of tumor-bearing mice (Fig. 4I). This effect was, however, only significant when mice were grafted with xCT WT Panc02 cells, and mainly driven by the $xCT^{-/-}$ mice (Fig. 4I). A similar trend was observed for another E3 ubiquitin ligase-related gene, Murf1 (Fig. 4J; borderline significance). Mafbx and Murf1 are targets of the Fox0 pathway, also involved in the regulation of the muscle mass (Reed et al., 2012). Yet, the expression of Foxo1 remained unchanged in the gastrocnemius muscle of tumor-bearing mice (Fig. 4K).

Taken together, our results show that targeting xCT in the tumor induces overall less hypothalamic inflammation, protects against muscle atrophy and increases food intake, while only targeting xCT in the host

cannot reproduce these effects.

3.4. Host xCT deletion results in attenuated anxiety- and depressive-like behavior in tumor-bearing mice

Deletion of host xCT did not significantly alter hippocampal cytokine mRNA levels (Supplementary Fig. S8A–C), nor the number or morphology of Iba-1^{+} (Supplementary methods and Fig. S8D–G) or GFAP^{+} cells (Supplementary methods and Fig. S8H–J). Despite the absence of statistical significance, in most of the above-mentioned analyses, higher levels of neuroinflammation were seen in the xCT$^{+/+}$ mice grafted with Panc02 WT cells, compared to xCT$^{-/-}$ mice. Moreover, while a positive correlation between TNF-α levels and tumor size was observed in mice grafted with xCT WT tumors, TNF-α levels decreased with an increasing size of xCT KO tumors (i.e. negative correlation; Supplementary Fig. S6B where only cytokines that significantly correlate with tumor size are shown). Finally, hippocampal xCT protein expression did not change with the genotype of the tumor (Supplementary Fig. S8L).

Importantly, eight to ten days after tumor cell injection (Fig. 5A), xCT$^{-/-}$ mice showed behavioral differences compared to xCT$^{+/+}$ mice. While they did not improve their nest building (Fig. 5B and C), xCT$^{-/-}$ mice did spend more time in the center of the open field compared to their xCT$^{+/+}$ littermates indicating attenuated anxiety-like behavior, an effect that is most obvious in xCT$^{-/-}$ mice injected with Panc02 WT cells (Fig. 5D). Locomotor activity in the open field test was not different between xCT$^{+/+}$ and xCT$^{-/-}$ mice (Fig. 5E and F) and thus did not bias other read-outs. Furthermore, a decreased immobility time of xCT$^{-/-}$ mice in the tail suspension test (Fig. 5G) underscores the reduced depressive-like behavior. Similarly, in the forced swim test, xCT$^{-/-}$ mice with WT tumor show reduced immobility compared to xCT$^{+/+}$ mice with WT tumor (Fig. 5H).

Taken together, in mice with pancreatic tumors, host xCT deletion reduces anxiety- and depressive-like behavior whereas only tumor xCT deletion did not show benefit.

4. Discussion

Over the past years, high tumor xCT expression has been correlated to poor patient survival in different cancer types (Briggs et al., 2016; Takeuchi et al., 2013; Ji et al., 2018; Kinoshita et al., 2013; Conti et al., 2020; Yang et al., 2020) and inhibition of system x_c^- was reported to be a valuable treatment strategy, due to its potential to reduce GSH synthesis and induce tumor cell death (for review (Jyotsana et al., 2022)). However, besides being upregulated in tumor cells, xCT is in physiological conditions mainly expressed on cells of the immune system and the brain, thereby modulating (neuro)inflammation and behavior (for review (Lewerenz et al., 2013; Massie et al., 2015)). In this study, we dissected the role of tumor, host and immune xCT expression in a mouse pancreatic cancer model. Tumor xCT deletion induced a strong reduction in tumor growth, it attenuated systemic and hypothalamic

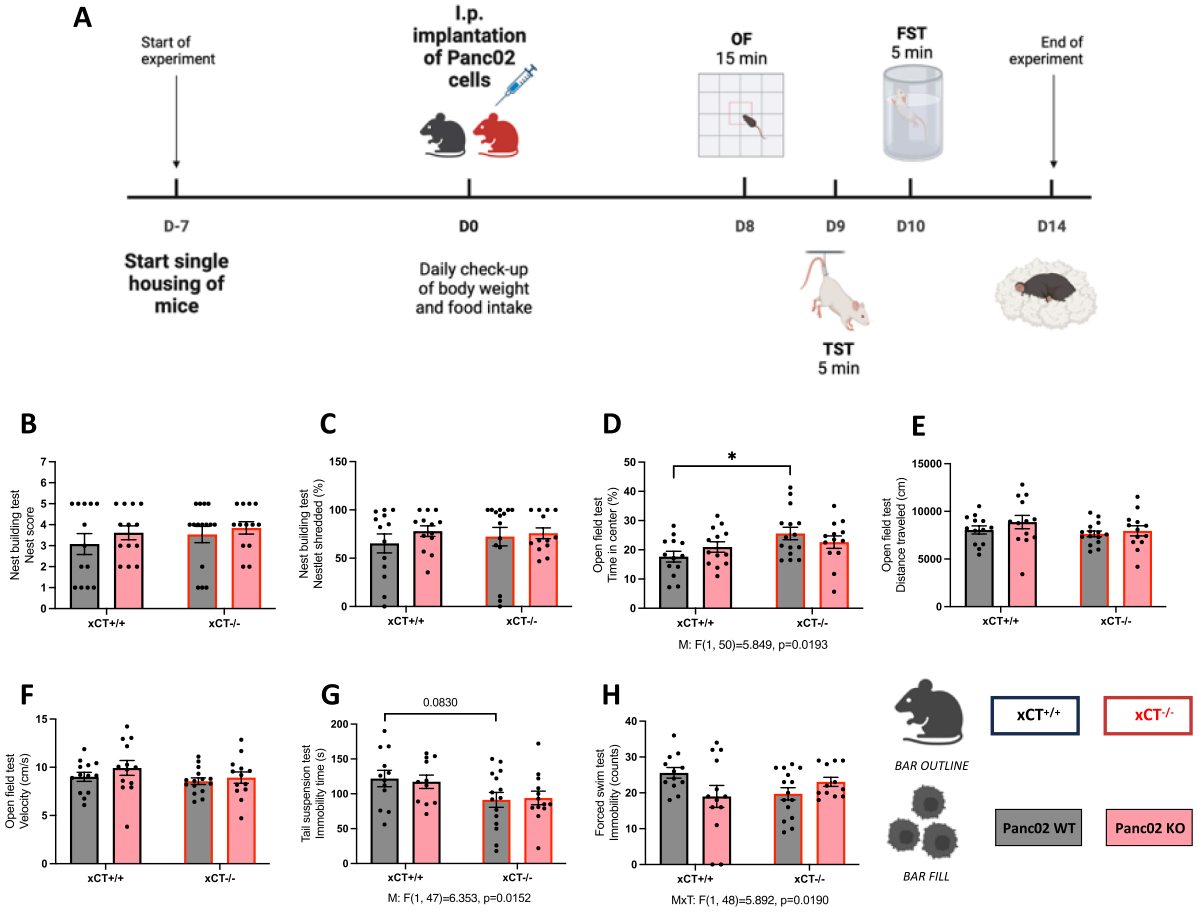

Fig. 5. Absence of host xCT reduces anxiety- and depressive-like behavior in tumor-bearing mice. A) *In vivo* experimental design to assess anxiety- and depressive-like behavior as well as general wellbeing, in xCT$^{+/+}$ and xCT$^{-/-}$ mice injected with Panc02 WT or Panc02 KO cells (n = 11–15 mice/group). B) Score of the nest and C) percentage of nest material shredded. D) Percentage of time spent in the center of an open field, E) distance traveled and F) velocity in the open field test. Immobility in G) the tail suspension test and H) forced swim test. Data are presented as mean ± SEM and were analyzed by a two-way ANOVA followed by Tukey's or Sidak's multiple comparisons test (B-H). Significant main effects of the two-way ANOVA are indicated below the graph: M mouse genotype effect, MxT interaction effect. Significant simple effects of the multiple comparisons test are indicated on the bars: *p < 0.05. Figure created with BioRender.com.

inflammation as well as early signs of muscle wasting, and it ameliorated food intake. Furthermore, we report that host xCT deletion was also beneficial in attenuating systemic inflammation and tumor-related mood disturbances, while only partially reducing tumor growth (Supplementary Fig. S9 for a comparative overview of the overall net effect of xCT tumor and host-induced effects). For some cytokines, the favorable effects of xCT deletion were mainly the result of reduced tumor size; yet, other cytokine levels were directly impacted by either mouse or tumor genotype, and not correlated to tumor size.

Using two mouse PDAC cell lines harboring the most frequently observed mutations in pancreatic cancer (Connor and Gallinger, 2022) but of different genetic make-up (Smad4 mutation in Panc02 cell line (Wang et al., 2012), Kras and p53 mutation in the KPC cell line (Morton et al., 2010)), we observed that xCT deletion inhibits *in vitro* tumor cell proliferation, in line with previous reports targeting xCT by a pharmacological or genetic approach in several PDAC cell lines (Arensman et al., 2019; Badgley et al., 2020; Daher et al., 2019; Lo et al., 2008). Despite the reported increase in xCT transcription by mutant KRAS (Hu et al., 2020; Lim et al., 2019), we detected higher xCT expression and increased system x_c^- - activity in Panc02 compared to KPC cells, and thus continued our *in vivo* experiments with the Panc02 cell line. We confirmed *in vivo* reduced growth of xCT deficient Panc02 cells, as previously reported (Arensman et al., 2019). While we did not pursue *in vivo* experiments with the KPC cells, others reported on xCT effects in KPC mice where systemic deletion of xCT extended survival (Badgley et al., 2020), while this was not seen when conditionally deleting xCT only in the epithelial cells of the pancreas (Sharbeen et al., 2021). Survival was thus only improved when xCT was targeted in both the tumor and stromal compartment, suggesting a crucial antitumorigenic role for xCT deletion in the stroma in the KPC model (Badgley et al., 2020).

Different from effects in the tumor microenvironment, host immune reactivity to cancer leads to chronic inflammation thereby inducing tumor progression and metastasis. Chronic inflammation was therefore shown to be predictive for poorer outcomes (for review (Kartikasari et al., 2021)). Our results highlight that not only deletion of xCT in the tumor but also host xCT deletion, attenuates peripheral inflammation. We previously reported a more efficient resolution of systemic inflammatory responses after LPS challenge in mice lacking xCT (Albertini et al., 2018), as well as reduced age-related priming of the inflammatory response to LPS (Verbruggen et al., 2022). Our current findings further support an emerging role for system x_c^- in modulating inflammatory responses in mice, that can be extended to cancer-related inflammation.

Although host xCT deletion without targeting xCT in the tumor exerted beneficial effects on systemic inflammation, its effect on tumor burden was reduced, in line with previous findings (Arensman et al., 2019). Interestingly, targeting xCT in the host and more specifically in macrophages, inhibited lung cancer growth and metastasis in mice (Tang et al., 2023). Yet, exclusive deletion of xCT from all immune cells did not reduce tumor burden in our experimental model. This discrepancy could be attributed to the fact that in PDAC xCT is mainly overexpressed in tumor cells, while for lung cancer, tumor-associated macrophages showed higher xCT expression levels compared to cancer cells (Tang et al., 2023). These findings once more underscore the need to disentangle the role of xCT in the different compartments to fully understand its function in different cancer types, as it might reveal a possible benefit of cell type-targeted xCT inhibition. Furthermore, our analysis of splenic immune cell populations in $xCT^{+/+}$ versus $xCT^{-/-}$ mice did not reveal changes in $CD4^+$ or $CD8^+$ populations, in line with previous observations by Arensman and colleagues (Arensman et al., 2019). However, the proportion of immunosuppressive Treg cells was increased in tumor-bearing $xCT^{+/+}$, and not $xCT^{-/-}$ mice. This effect was reproduced by exclusive deletion of xCT on immune cells, suggesting a role for Treg xCT expression in cancer, as was reported in a model of relapsing-remitting multiple sclerosis where oxidative stress in Treg cells was prevented by xCT expression and thus enhanced Treg cell proliferation (Procaccini et al., 2021). Tumor xCT expression was also shown to support Treg suppressive functions in a glioblastoma model, as a result of glutamate release leading to Treg cell proliferation and activation (Long et al., 2020). Of note, the use of cryopreserved samples (compared to fresh samples) in our study could raise concerns since it was reported to affect certain immune cell populations, such as for example T cells (Li et al., 2022). Yet, the cryopreservation medium used here ensures the stability of peripheral blood mononuclear cells (Safinia et al., 2016; Kofanova et al., 2014).

Altogether, our findings on tumor growth after deleting xCT on tumor cells, immune cells or in the host, show that tumor xCT deletion is required to effectively reduce tumor burden, while beneficial effects on peripheral inflammation and immunosuppression are achieved by host xCT deletion, even when the tumor expresses xCT. Since specific xCT deletion in immune cells did not attenuate peripheral inflammation, other host cell types must be responsible for this effect in $xCT^{-/-}$ mice. The endothelial cells -the population with the second highest xCT expression in human PDAC- could possibly be involved by regulating the infiltration of leukocytes (Pober and Sessa, 2007) and/or by releasing cytokines (Mai et al., 2013). We have indeed unpublished findings -that require further investigation- on a very limited number of samples, showing that immune cell infiltration in the tumor is strongly reduced in tumor-bearing $xCT^{-/-}$ mice compared to $xCT^{+/+}$ mice, independent of the genotype of the tumor.

We here show that $xCT^{+/+}$ mice injected with Panc02 WT cells showed a strong increase in plasma IL-6 levels, in analogy with findings of Greco *et al.* (Greco et al., 2015), while xCT deletion diminished this effect. As systemic mediators of inflammation can induce an inflammatory response in the central nervous system (Santos and Pyter, 2018; Sun et al., 2022), tumor xCT deletion indeed resulted in reduced hypothalamic mRNA expression of TNF-α and IL-6, two pro-inflammatory cytokines. The attenuated peripheral and central inflammation in our model -either directly or indirectly as a consequence of smaller tumors- suggests that tumor xCT deletion might have protective effects in cachexia (for review (Henderson et al., 2018)). Although not all mice in our study developed cachexia -probably due to our experimental timeline that was designed to ensure behavioral analyses would be finalized and mice sacrificed before humane endpoints would be reached- we did observe increased food intake and attenuated expression of muscle catabolism genes when xCT was deleted in tumor cells. Interestingly, current therapeutic strategies for cachexia aim at targeting peripheral inflammation and, more specifically, anti-IL-6 treatment in non-small cell lung cancer patients successfully ameliorated cachexia (for review (Argilés et al., 2019)). We here provide for the first time evidence that deletion of xCT in the tumor strongly attenuates (hypothalamic) inflammation and some markers of muscle catabolism, and preserves food intake, thus putting xCT forward as a possible target to prevent cachexia. However, this should further be evaluated in an experimental setup that is specifically designed for assessing pancreatic cancer cachexia.

By modulating (neuro)inflammation, xCT deletion was shown to diminish LPS-induced depressive-like behavior in adult mice (Albertini et al., 2018), and healthy adult and aged $xCT^{-/-}$ mice show reduced anxiety- and depressive-like behavior compared to age-matched $xCT^{+/+}$ controls (Bentea et al., 2015). While we only observed minor effects on hippocampal inflammation, it became very apparent that $xCT^{-/-}$ mice with an xCT expressing tumor showed reduced anxiety- and depressive-like behavior, compared to their wildtype littermates. Importantly, this was not merely the result of reduced tumor growth as host xCT deletion -needed to obtain beneficial effects in behavior- only partly reduced tumor burden compared to the strong effect observed by tumor xCT deletion. A possible explanation is that xCT -the major source of extracellular glutamate in several brain regions (Massie et al., 2015)- modulates glutamatergic signaling in the hippocampus (De Bundel et al., 2011), which is hypothesized to be disturbed in patients with mood disorders (Popoli et al., 2011). While we did not see increased hippocampal xCT expression in tumor-bearing mice, genetic xCT deletion will

reduce extracellular glutamate levels (De Bundel et al., 2011) and as such counter aberrant activation of (extrasynaptic) glutamate receptors.

To conclude, we here report for the first time that targeting xCT in pancreatic cancer has beneficial effects in the periphery and in the central nervous system. Together this leads to attenuated cancer-related comorbidities, beyond direct growth inhibition of the tumor. Indeed, although reduced peripheral inflammation was mainly the result of reduced KO tumor growth, the impact of tumor weight was very limited in the brain, yet there was reduced neuroinflammation. In essence, from a clinical point of view, it is the sum of the effects that patients will benefit from when being treated with system x_c^- inhibitors and thus overall inhibition of system x_c^- could be a valuable multi-faceted approach to treat pancreatic cancer. In addition, in patients with a low xCT expressing tumor (see the variability in expression among the patients, Fig. 1A), targeting of xCT could thus still be beneficial based on its peripheral and central effects that are unrelated to tumor xCT expression. The lack of effect of SAS in this context compels the development of new and specific system x_c^- inhibitors that could also cross the blood–brain barrier as a promising therapy for pancreatic cancer.

Funding

This work was supported by Kom Op Tegen Kanker (ANI219 to AM and IR), a Strategic Research Program of the Vrije Universiteit Brussel (SRP49 to AM), the Scientific Fund Willy Gepts (WFWG – UZ Brussel to PJ), G001619N project from Fund for Scientific Research Flanders (FWO to IR) and the Oncology Research Center (Vrije Universiteit Brussel to PJ). OL, LDP, JW and GA are supported by the FWO (Aspirant fellowship 11C2719N to OL, 11658ON to LPD and 11PRE24N to JW; postdoctoral fellowship 12B3223N to GA). IR was supported by an FWO Odysseus Fellowship G0F8916N.

CRediT authorship contribution statement

Olaya Lara: Conceptualization, Formal analysis, Investigation, Methodology, Writing – original draft. **Pauline Janssen:** Conceptualization, Formal analysis, Investigation, Methodology, Writing – original draft. **Marco Mambretti:** Investigation, Methodology, Writing – review & editing. **Laura De Pauw:** Investigation, Writing – review & editing. **Gamze Ates:** Investigation, Methodology, Writing – review & editing. **Liselotte Mackens:** Investigation, Writing – review & editing. **Jolien De Munck:** Investigation, Writing – review & editing. **Jarne Walckiers:** Investigation, Writing – review & editing. **Zhaolong Pan:** Investigation, Writing – review & editing. **Pauline Beckers:** Investigation, Writing – review & editing. **Elisa Espinet:** Investigation, Methodology, Writing – review & editing. **Hideyo Sato:** Resources, Writing – review & editing. **Mark De Ridder:** Methodology, Resources, Writing – review & editing. **Daniel L. Marks:** Methodology, Writing – review & editing. **Kurt Barbé:** Formal analysis, Methodology, Writing – review & editing. **Joeri L. Aerts:** Methodology, Writing – review & editing. **Emmanuel Hermans:** Methodology, Resources, Writing – review & editing. **Ilse Rooman:** Conceptualization, Formal analysis, Funding acquisition, Project administration, Resources, Supervision, Writing – original draft. **Ann Massie:** Conceptualization, Formal analysis, Funding acquisition, Project administration, Resources, Supervision, Writing – original draft.

Declaration of Competing Interest

The authors declare that they have no known competing financial interests or personal relationships that could have appeared to influence the work reported in this paper.

Data availability

Data will be made available on request.

Acknowledgments

We kindly thank Frank Van der Kelen (Vrije Universiteit Brussel, Belgium), Prof. Thierry Gevaert (Department of Radiotherapy, UZ Brussels, Belgium) and the FlowCore facility of the VUB for their technical assistance.

Appendix A. Supplementary data

Supplementary data to this article can be found online at https://doi.org/10.1016/j.bbi.2024.03.001.

References

Albertini, G., Deneyer, L., Ottestad-Hansen, S., Zhou, Y., Ates, G., Walrave, L., et al., 2018. Genetic deletion of xCT attenuates peripheral and central inflammation and mitigates LPS-induced sickness and depressive-like behavior in mice. Glia 66 (9), 1845–1861.
Angelini, G., Gardella, S., Ardy, M., Ciriolo, M.R., Filomeni, G., Di Trapani, G., et al., 2002. Antigen-presenting dendritic cells provide the reducing extracellular microenvironment required for T lymphocyte activation. PNAS 99 (3), 1491–1496.
Arensman, M.D., Yang, X.S., Leahy, D.M., Toral-Barza, L., Mileski, M., Rosfjord, E.C., et al., 2019. Cystine–glutamate antiporter xCT deficiency suppresses tumor growth while preserving antitumor immunity. PNAS 116 (19), 9533–9542.
Argilés, J.M., López-Soriano, F.J., Stemmler, B., Busquets, S., 2019. Therapeutic strategies against cancer cachexia. Eur J Transl Myol. 29 (1), 7960.
Badgley, MA, Kremer, DM, Maurer, HC, Delgiorno, KE, Lee, HJ, Purohit, V, et al., 2020. Cysteine depletion induces pancreatic tumor ferroptosis in mice. Science 368 (6486), 85–89.
Beckers, P., Lara, O., Belo do Nascimento, I., Desmet, N., Massie, A., Hermans, E., 2022. Validation of a system xc– functional assay in cultured astrocytes and nervous tissue samples. Front. Cell. Neurosci. 15, 815771.
Bentea, E., Demuyser, T., Van Liefferinge, J., Albertini, G., Deneyer, L., Nys, J., et al., 2015. Absence of system xc- in mice decreases anxiety and depressive-like behavior without affecting sensorimotor function or spatial vision. Prog. Neuropsychopharmacol. Biol. Psychiatry (59), 49–58.
Briggs, K.J., Koivunen, P., Cao, S., Backus, K.M., Olenchock, B.A., Patel, H., et al., 2016. Paracrine Induction of HIF by Glutamate in Breast Cancer: EglN1 Senses Cysteine. Cell 166 (1), 126–139.
Chandra, D., Selvanesan, B.C., Yuan, Z., Libutti, S.K., Koba, W., Beck, A., et al., 2017. 32-Phosphorus selectively delivered by listeria to pancreatic cancer demonstrates a strong therapeutic effect. Oncotarget 8 (13), 20729–20740.
Connor, A.A., Gallinger, S., 2022. Pancreatic cancer evolution and heterogeneity: integrating omics and clinical data. Nat. Rev. Cancer 22 (3), 131–142.
Conti, L., Bolli, E., di Lorenzo, A., Franceschi, V., Macchi, F., Riccardo, F., et al., 2020. Immunotargeting of the xCT Cystine/Glutamate Antiporter Potentiates the Efficacy of HER2-Targeted Immunotherapies in Breast Cancer. Cancer Immunol. Res. 8 (8), 1039–1053.
Daher, B., Parks, S.K., Durivault, J., Cormerais, Y., Baidarjad, H., Tambutte, E., et al., 2019. Genetic ablation of the cystine transporter xCT in PDAC cells inhibits mTORC1, growth, survival, and tumor formation via nutrient and oxidative stresses. Cancer Res. 79 (15), 3877–3890.
Dantzer, R., 2006. Cytokine, sickness behavior, and depression. Neurol. Clin. 24 (3), 441–460.
Davis, N.E., Hue, J.J., Kyasaram, R.K., Elshami, M., Graor, H.J., Zarei, M., et al., 2022. Prodromal depression and anxiety are associated with worse treatment compliance and survival among patients with pancreatic cancer. Psychooncology 31 (8), 1390–1398.
De Bundel, D., Schallier, A., Loyens, E., Fernando, R., Miyashita, H., Van Liefferinge, J., et al., 2011. Loss of system x(c)- does not induce oxidative stress but decreases extracellular glutamate in hippocampus and influences spatial working memory and limbic seizure susceptibility. J. Neurosci. 31 (15), 5792–5803.
Deacon, R.M.J., 2006. Assessing nest building in mice. Nat. Protoc. 1 (3), 1117–1119.
Espinet, E., Gu, Z., Imbusch, C.D., Giese, N.A., Büscher, M., Safavi, M., et al., 2021. Aggressive PDACs Show Hypomethylation of Repetitive Elements and the Execution of an Intrinsic IFN Program Linked to a Ductal Cell of Origin. Cancer Discov. 11 (3), 638–659.
Foley, K., Rucki, A.A., Xiao, Q., Zhou, D., Leubner, A., Mo, G., et al., 2015. Semaphorin 3D autocrine signaling mediates the metastatic role of annexin A2 in pancreatic cancer. Sci. Signal. 8 (388), ra77.
Greco, S.H., Tomkötter, L., Vahle, A.K., Rokosh, R., Avanzi, A., Mahmood, S.K., et al., 2015. TGF-β Blockade Reduces Mortality and Metabolic Changes in a Validated Murine Model of Pancreatic Cancer Cachexia. PLoS One 10 (7), e0132786.
Grossberg, A.J., Scarlett, J.M., Marks, D.L., 2010. Hypothalamic mechanisms in cachexia. Physiol. Behav. 100 (5), 478–489.
Henderson, S.E., Makhijani, N., Mace, T.A., 2018. Pancreatic Cancer-Induced Cachexia and Relevant Mouse Models. Pancreas 47 (8), 937–945.
Hu, K., Li, K., Lv, J., Feng, J., Chen, J., Wu, H., et al., 2020. Suppression of the SLC7A11/glutathione axis causes synthetic lethality in KRAS-mutant lung adenocarcinoma. J. Clin. Invest. 130 (4), 1752–1766.
Janssen, P., De Pauw, L., Mambretti, M., Lara, O., Walckiers, J., Mackens, L., et al., 2023. Characterization of the long-term effects of lethal total body irradiation followed by

bone marrow transplantation on the brain of C57BL/6 mice. Int. J. Radiat Biol. 17, 1–14.
Ji, X., Qian, J., Rahman, S.M.J., Siska, P.J., Zou, Y., Harris, B.K., et al., 2018. xCT (SLC7A11)-mediated metabolic reprogramming promotes non-small cell lung cancer progression. Oncogene 37 (36), 5007–5019.
Jyotsana, N., Ta, K.T., DelGiorno, K.E., 2022. The Role of Cystine/Glutamate Antiporter SLC7A11/xCT in the Pathophysiology of Cancer. Front. Oncol. 12, 858462.
Kartikasari, A.E.R., Huertas, C.S., Mitchell, A., Plebanski, M., 2021. Tumor-Induced Inflammatory Cytokines and the Emerging Diagnostic Devices for Cancer Detection and Prognosis. Front. Oncol. 11, 692142.
Kinoshita, H., Okabe, H., Beppu, T., Chikamoto, A., Hayashi, H., Imai, K., et al., 2013. Cystine/glutamic acid transporter is a novel marker for predicting poor survival in patients with hepatocellular carcinoma. Oncol. Rep. 29 (2), 685–689.
Kleeff, J., Korc, M., Apte, M., La Vecchia, C., Johnson, C.D., Biankin, A.V., et al., 2016. Pancreatic Cancer. Nat Rev Dis Primers. 21 (2), 16022.
Kofanova, O.A., Davis, K., Glazer, B., De Souza, Y., Kessler, J., Betsou, F., et al., 2014. Viable mononuclear cell stability study for implementation in a proficiency testing program: impact of shipment conditions. Biopreserv Biobank. 12 (3), 206–216.
Lee, C.H., Giuliani, F., 2019. The Role of Inflammation in Depression and Fatigue. Front. Immunol. 10, 1696.
Levring, T.B., Hansen, A.K., Nielsen, B.L., Kongsbak, M., von Essen, M.R., Woetmann, A., et al., 2012. Activated human CD4+ T cells express transporters for both cysteine and cystine. Sci. Rep. 2, 266.
Lewerenz, J., Hewett, S.J., Huang, Y., Lambros, M., Gout, P.W., Kalivas, P.W., et al., 2013. The cystine/glutamate antiporter system xc- in health and disease: From molecular mechanisms to novel therapeutic opportunities. Antioxid. Redox Signal. 18, 522–555.
Li, B., Yang, C., Jia, G., Liu, Y., Wang, N., Yang, F., et al., 2022. Comprehensive evaluation of the effects of long-term cryopreservation on peripheral blood mononuclear cells using flow cytometry. BMC Immunol. 23 (1), 30.
Lim, J.K.M., Delaidelli, A., Minaker, S.W., Zhang, H.F., Colovic, M., Yang, H., et al., 2019. Cystine/glutamate antiporter xCT (SLC7A11) facilitates oncogenic RAS transformation by preserving intracellular redox balance. PNAS 116 (19), 9433–9442.
Lippi, G., Mattiuzzi, C., 2020. The global burden of pancreatic cancer. Arch. Med. Sci. 16 (4), 820–824.
Lo, M., Wang, Y.Z., Gout, P.W., 2008. The x(c)- cystine/glutamate antiporter: a potential target for therapy of cancer and other diseases. J. Cell. Physiol. 215 (3), 593–602.
Lo, M., Ling, V., Wang, Y.Z., Gout, P.W., 2008. The xc- cystine/glutamate antiporter: A mediator of pancreatic cancer growth with a role in drug resistance. Br. J. Cancer 99 (3), 464–472.
Long, Y., Tao, H., Karachi, A., Grippin, A.J., Jin, L., Chang, Y.E., et al., 2020. Dysregulation of Glutamate Transport Enhances Treg Function That Promotes VEGF Blockade Resistance in Glioblastoma. Cancer Res. 80 (3), 499–509.
Mai, J., Virtue, A., Shen, J., Wang, H., Yang, X.F., 2013. An evolving new paradigm: endothelial cells–conditional innate immune cells. J. Hematol. Oncol. 22 (6), 61.
Massie, A., Schallier, A., Kim, S.W., Fernando, R., Kobayashi, S., Beck, H., et al., 2011. Dopaminergic neurons of system x c − -deficient mice are highly protected against 6-hydroxydopamine-induced toxicity. FASEB J. 25 (4), 1359–1369.
Massie, A., Boillée, S., Hewett, S., Knackstedt, L., Lewerenz, J., 2015. Main path and byways: Non-vesicular glutamate release by system xc- as an important modifier of glutamatergic neurotransmission. J. Neurochem. 135 (6), 1062–1079.
Michaelis, K.A., Zhu, X., Burfeind, K.G., Krasnow, S.M., Levasseur, P.R., Morgan, T.K., et al., 2017. Establishment and characterization of a novel murine model of pancreatic cancer cachexia. J. Cachexia. Sarcopenia Muscle 8 (5), 824–838.
Mizrahi, J.D., Surana, R., Valle, J.W., Shroff, R.T., 2020. Pancreatic cancer. Lancet 395 (10242), 2008–2020.
Morton, J.P., Timpson, P., Karim, S.A., Ridgway, R.A., Athineos, D., Doyle, B., et al., 2010. Mutant p53 drives metastasis and overcomes growth arrest/senescence in pancreatic cancer. PNAS 107 (1), 246–251.
Nashed, M.G., Ungard, R.G., Young, K., Zacal, N.J., Seidlitz, E.P., Fazzari, J., et al., 2017. Behavioural effects of using sulfasalazine to inhibit glutamate released by cancer cells: A novel target for cancer-induced depression. Sci. Rep. 25, 7.
Pober, J.S., Sessa, W.C., 2007. Evolving functions of endothelial cells in inflammation. Nat. Rev. Immunol. 7 (10), 803–815.
Popoli, M., Yan, Z., McEwen, B.S., Sanacora, G., 2011. The stressed synapse: the impact of stress and glucocorticoids on glutamate transmission. Nat. Rev. Neurosci. 13 (1), 22–37.
Poulia, K.A., Sarantis, P., Antoniadou, D., Koustas, E., Papadimitropoulou, A., Papavassiliou, A.G., et al., 2020. Pancreatic Cancer and Cachexia-Metabolic Mechanisms and Novel Insights. Nutrients 12 (6), 1543.
Procaccini, C., Garavelli, S., Carbone, F., di Silvestre, D., la Rocca, C., Greco, D., et al., 2021. Signals of pseudo-starvation unveil the amino acid transporter SLC7A11 as key determinant in the control of Treg cell proliferative potential. Immunity 54 (7), 1543–1560.e6.
Reed, S.A., Sandesara, P.B., Senf, S.M., Judge, A.R., 2012. Inhibition of FoxO transcriptional activity prevents muscle fiber atrophy during cachexia and induces hypertrophy. FASEB J. 26 (3), 987–1000.
Safinia, N., Vaikunthanathan, T., Fraser, H., Thirkell, S., Lowe, K., Blackmore, L., et al., 2016. Successful expansion of functional and stable regulatory T cells for immunotherapy in liver transplantation. Oncotarget 7 (7), 7563–7577.
Santos, J.C., Pyter, L.M., 2018. Neuroimmunology of Behavioral Comorbidities Associated With Cancer and Cancer Treatments. Front. Immunol. 9, 1195.
Sato, H., Shiiya, A., Kimata, M., Maebara, K., Tamba, M., Sakakura, Y., et al., 2005. Redox imbalance in cystine/glutamate transporter-deficient mice. J. Biol. Chem. 280 (45), 37423–37429.
Sharbeen, G., McCarroll, J.A., Akerman, A., Kopecky, C., Youkhana, J., Kokkinos, J., et al., 2021. Cancer-Associated Fibroblasts in Pancreatic Ductal Adenocarcinoma Determine Response to SLC7A11 Inhibition. Cancer Res. 81 (13), 3461–3479.
Siska, P.J., Kim, B., Ji, X., Hoeksema, M.D., Massion, P.P., Beckermann, K.E., et al., 2016. Fluorescence-based measurement of cystine uptake through xCT shows requirement for ROS detoxification in activated lymphocytes. J. Immunol. Methods 438, 51–58.
Srivastava, M.K., Sinha, P., Clements, V.K., Rodriguez, P., Ostrand-Rosenberg, S., 2010. Myeloid-derived suppressor cells inhibit T-cell activation by depleting cystine and cysteine. Cancer Res. 70 (1), 68–77.
Starheim, K.K., Holien, T., Misund, K., Johansson, I., Baranowska, K.A., Sponaas, A.M., et al., 2016. Intracellular glutathione determines bortezomib cytotoxicity in multiple myeloma cells. Blood Cancer J. 6 (7), e446.
Sun, Y., Koyama, Y., Shimada, S., 2022. Inflammation From Peripheral Organs to the Brain: How Does Systemic Inflammation Cause Neuroinflammation? Front. Aging Neurosci. 14, 903455.
Takeuchi, S., Wada, K., Toyooka, T., Shinomiya, N., Shimazaki, H., Nakanishi, K., et al., 2013. Increased xCT expression correlates with tumor invasion and outcome in patients with glioblastomas. Neurosurgery 72 (1), 33–41.
Tan, C.R., Yaffee, P.M., Jamil, L.H., Lo, S.K., Nissen, N., Pandol, S.J., et al., 2014. Pancreatic Cancer Cachexia: A Review of Mechanisms and Therapeutics, 5. Frontiers in Physiology 5, 88., p. 88
Tang, B., Wang, Y., Xu, W., Zhu, J., Weng, Q., Chen, W., et al., 2023. Macrophage xCT deficiency drives immune activation and boosts responses to immune checkpoint blockade in lung cancer. Cancer Lett. 1 (554), 216021.
Van Liefferinge, J., Bentea, E., Demuyser, T., Albertini, G., Follin-Arbelet, V., Holmseth, S., et al., 2016. Comparative analysis of antibodies to xCT (Slc7a11): Forewarned is forearmed. J Comp Neurol 524 (5), 1015–1032.
Verbruggen, L., Ates, G., Lara, O., De Munck, J., Villers, A., De Pauw, L., et al., 2022. Lifespan extension with preservation of hippocampal function in aged system xc−-deficient male mice. Mol. Psychiatry 27 (4), 2355–2368.
Wang, S.F., Chen, M.S., Chou, Y.C., Ueng, Y.F., Yin, P.H., Yeh, T.S., et al., 2016. Mitochondrial dysfunction enhances cisplatin resistance in human gastric cancer cells via the ROS-activated GCN2-eIF2α-ATF4-xCT pathway. Oncotarget 7 (45), 74132–74151.
Wang, Y., Zhang, Y., Yang, J., Ni, X., Liu, S., Li, Z., et al., 2012. Genomic sequencing of key genes in mouse pancreatic cancer cells. Curr. Mol. Med. 12 (3), 331–341.
Yang, Q., Li, K., Huang, X., Zhao, C., Mei, Y., Li, X., et al., 2020. lncRNA SLC7A11-AS1 Promotes Chemoresistance by Blocking SCFβ-TRCP-Mediated Degradation of NRF2 in Pancreatic Cancer. Mol. Ther. Nucleic Acids 6 (19), 974–985.
Zhang, P., Wang, W., Wei, Z., Xu, L.I., Yang, X., Du y., 2016. xCT expression modulates cisplatin resistance in Tca8113 tongue carcinoma cells. Oncol. Lett. 12 (1), 307–314.
Zimmers, T.A., Fishel, M.L., Bonetto, A., 2016. STAT3 in the systemic inflammation of cancer cachexia. In: Semin Cell Dev Biol., 54, pp. 28–41.